Available online at www.sciencedirect.com

SciVerse ScienceDirect

Ceramics International 39 (2013) 5943–5948

CERAMICS INTERNATIONAL

www.elsevier.com/locate/ceramint

Short communication

Microwave dielectric properties and low sintering temperature of $Ba_{0.5}Sr_{0.5}TiO_3$–Mg_2TiO_4 composites synthesized in situ by the hydrothermal method

Jingji Zhang[a,b,c], Bo Shen[b], Jiwei Zhai[a,b,*], Xi Yao[b]

[a]Shanghai Key Laboratory of Special Artificial Microstructure Materials and Technology, Tongji University, 1239 Siping Road, Shanghai, China
[b]Functional Materials Research Laboratory, Tongji University, 1239 Siping Road, Shanghai, China
[c]College of Materials Science and Engineering, China Jiliang University, 258 Xueyuan Street, Hangzhou, China

Received 31 October 2012; received in revised form 23 November 2012; accepted 23 November 2012
Available online 3 December 2012

Abstract

$(1-x)Ba_{0.5}Sr_{0.5}TiO_3$–$xMg_2TiO_4$ composite ceramics were synthesized in situ by the hydrothermal method and their structure and dielectric properties were investigated systematically. Results showed that a ferroelectric–dielectric composite containing $Ba_{0.5}Sr_{0.5}TiO_3$ and Mg_2TiO_4 phases could be successfully synthesized at sintering temperatures below 1300 °C. As the sintering temperature increased, the dielectric peaks of the cubic-tetragonal phase transition were markedly enhanced and sharpened and shifted toward high temperature. As the concentration of Mg_2TiO_4 increased, both permittivity (ε) and tunability (T) decreased, whereas Q value firstly increased and then decreased. The sample with $x=0.6$ exhibited good microwave dielectric properties, with ε of 136, Q of 342 (at 3.804 GHz) and T of 16.2%, which make it a potential candidate for the fabrication of tunable microwave devices.

Keywords: Composite ceramics; Hydrothermal method; Tunability; Microwave dielectric properties

1. Introduction

$Ba_{1-x}Sr_xTiO_3$ (BST) has attracted significant interest due to its electrically tunable dielectric properties for potential applications in wireless telecommunications, as tunable mixers, delay lines, filters and phase shifters for steerable antennas [1]. As the work frequency of microwave components increases, it is essential to research a material with low permittivity (ε), low dissipation factor ($\tan\delta$) and moderate tunability, which is expected to come true by introducing low-permittivity dielectrics into BSTs. Researchers usually improve the dielectric properties of BST-based compounds by modifying their composition using the traditional solid-state method [2–6]. Recently, it has been found that the dielectric properties of BST-based composite ceramics could also be modified or controlled by their microstructure [7–10]. Therefore, increased attention has been paid on the preparations. Such as using the heterogeneous precipitation method [7] and chemical coating method [8] make BST system randomly dispersed by low-permittivity dielectric phases. It was reported that the $Ba_{0.55}Sr_{0.45}TiO_3$/MgO composites prepared by the heterogeneous precipitation method exhibited a small grain size, uniform microstructure, high tunability, and low microwave loss [7]. The hydrothermal process is one of the commonly used methods for preparing nanoscaled powders with good dispersion and narrow particles distribution. However, little attempt has been made to prepare BST-based composite ceramics by using the hydrothermal process.

In our previous work, BST-based composite ceramics was obtained by the conventional "two step" method. Low-permittivity dielectric phases was firstly formed and then added into BST phase to form the BST-based composite ceramics, which raised their microwave loss

*Corresponding author at: Shanghai Key Laboratory of Special Artificial Microstructure Materials and Technology, Tongji University, 1239 Siping Road, Shanghai, China. Tel.: +86 21 65980544; fax: +86 21 65985179.
E-mail address: apzhai@tongji.edu.cn (J. Zhai).

0272-8842/$ - see front matter © 2012 Elsevier Ltd and Techna Group S.r.l. All rights reserved.
http://dx.doi.org/10.1016/j.ceramint.2012.11.089

due to the formation of undesired phases [11] and the occurrence of structural disordering [12,13]. Herein, $(1-x)Ba_{0.5}Sr_{0.5}TiO_3$–$xMg_2TiO_4$ composite ceramics were synthesized in situ by the hydrothermal method and their structure and dielectric properties were systemically investigated.

2. Experimental procedure

0.03 mol of $(1-x)Ba_{0.5}Sr_{0.5}TiO_3$–$xMg_2TiO_4$ powders were synthesized by the hydrothermal process using Ba$(CH_3COO)_2$ (99.0%), Sr$(CH_3COO)_2$ (98.0%), Mg$(CH_3COO)_2$ (99.0%), $C_{16}H_{36}O_4Ti$ (99.8%), $C_5H_8O_2$ (99.8%) and KOH (99.8%) starting materials. According to the stoichiometric ratio $(1-x)Ba_{0.5}Sr_{0.5}TiO_3$–$xMg_2TiO_4$ with $x=0.5$, 0.6 and 0.7, Ba$(CH_3COO)_2$, Sr$(CH_3COO)_2$ and Mg$(CH_3COO)_2$ were dissolved into 60 mL deionized water. Meanwhile, 0.03 mol of $C_{16}H_{36}O_4Ti$ was mixed with 0.06 mol of $C_5H_8O_2$ to form a yellowish solution. The above two solutions were mixed to form a Ba–Sr–Mg–Ti solution. With stirring, 100 mL of 3 M KOH solution was slowly added into the previously prepared Ba–Sr–Mg–Ti solution. The precursors were transferred into a 200 mL Teflon-lined stainless steel reactor, sealed and then heated at 180 °C for 24 h. After reaction, the autoclave was allowed to cool down room temperature. The as-synthesized powders were filtrated and washed with deionized water and ethanol to remove the remaining ions and then dried at 100 °C for 6 h. After drying, the powders were annealed at 500 °C for 4 h. The annealed powders, mixed with 8 wt% polyvinyl alcohol, were pressed into pellets at 100 MPa. The gree pellets were kept at 550 °C for 6 h to remove the solvent as well as the binder and then sintered at different temperatures for 4 h.

Crystal structure of the obtained samples was identified by means of X-ray diffraction (XRD, Bruker D8 advanced, Germany) with Cu$K\alpha$ radiation. Fourier transform infrared spectra were characterized by Fourier transform infrared spectroscopy (FTIR, Brukeer Tensor27, Germany) to support the XRD results. A differential thermal analysis (DSC/TG, Model Netzsch STA449C, Germany) was performed to investigate the thermal decomposition behavior of the as-synthesized powders. Microstructural information was obtained by using a scanning electron microscopy (SEM, JSM EMP -800). Permittivity as a function of temperature was measured at different frequencies in the temperature range of −150 °C to 125 °C, using a HP4284A precision LCR meter (Agilent, Palo Alto, CA). Room temperature permittivity vs. DC bias voltage was measured at 10 kHz by using a Keithley model 2410 (Cleveland, OH) high-voltage source coupled with a TH2816A LCR meter (Changzhou, China). The permittivity ε and Q value at microwave frequencies were measured by the resonance method using a vector network analyzer (Agilent E5071C).

3. Results and discussion

XRD patterns of the $(1-x)Ba_{0.5}Sr_{0.5}TiO_3$–$xMg_2TiO_4$ powders synthesized by the hydrothermal method are shown in Fig. 1. The sample with $x=0.5$ shows a multiphase structure of BST, $Mg(OH)_2$, $MgTiO_3$ and $Ba_6Ti_{17}O_{40-x}$. As x increases, BST diffraction peaks are markedly weakened and broadened, indicating that the nucleation ability of BST becomes weak with increasing the molar ratio of (Ba+Sr+Mg)/KOH. Meanwhile, $Mg(OH)_2$ diffraction peaks are slightly weakened and broadened.

The formation of BST, $Mg(OH)_2$, $MgTiO_3$ and $Ba_6Ti_{17}O_{40-x}$ is further supported by FTIR spectra as shown in Fig. 2. All spectra have a sharp and intense peak at ~3698 cm^{-1}, which is attributed to the O–H stretching vibration in the crystal structure [14], indicating the

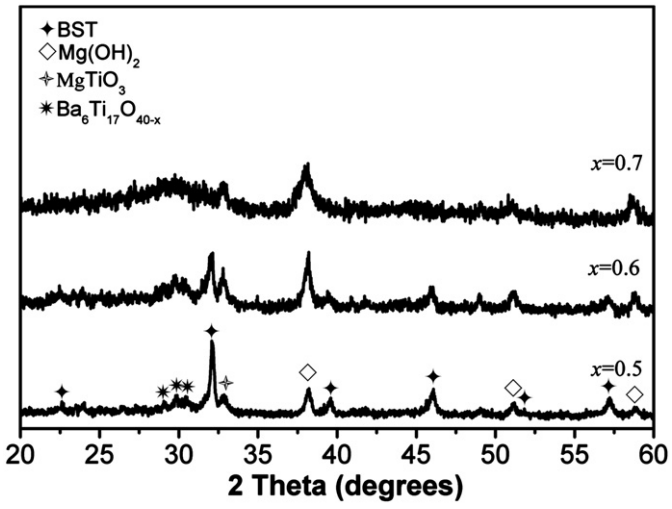

Fig. 1. XRD patterns of the $(1-x)Ba_{0.5}Sr_{0.5}TiO_3$–$xMg_2TiO_4$ powders synthesized by the hydrothermal method.

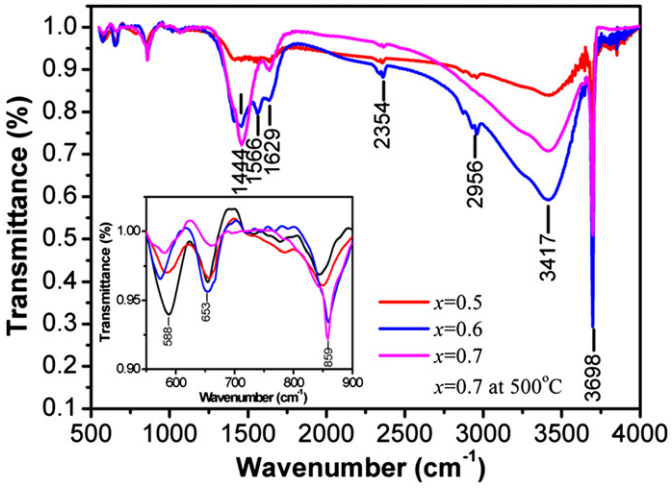

Fig. 2. FTIR spectra of the as-synthesized $(1-x)Ba_{0.5}Sr_{0.5}TiO_3$–$xMg_2TiO_4$ powders and the powders after the heat treatment at 500 °C for 4 h.

existence of $Mg(OH)_2$ phase. The absorption peaks at $\sim$3417 cm^{-1} and $\sim$1629 cm^{-1} are the O–H stretching vibration of the residual water and organic substances [15]. As x increases, the absorption peaks at $\sim$3417 cm^{-1} and $\sim$1629 cm^{-1} become stronger and stronger, whereas those get weak after the heat treatment at 500 °C. According to [16], the absorption peaks at 1550–1590 cm^{-1} and 1430–1470 cm^{-1} are attributable to the bidentate of Ti–carboxylic complexes. The latter is overlapped by the scissoring frequency of $–CH_2–$ at 1464 cm^{-1} and, consequently, forms a broad peak. The absorption peaks at $\sim$1566 cm^{-1} and $\sim$1444 cm^{-1} indicate that the Ti–carboxylic complexes are formed in the sample with $x=0.7$. After the heat treatment at 500 °C, the two peaks are amalgamated into a broad and strong peak. The peaks in the low wavenumber range (400–1000 cm^{-1}) correspond to the Ti–O vibrations [17]. The absorption peak at $\sim$859 cm^{-1} is probably the Ti–O stretching vibration in $MgTiO_3$. The absorption peak between 500 cm^{-1} and 700 cm^{-1} is the characteristic vibration frequency of TiO_6 octahedra [18]. All FTIR spectra strongly confirm our XRD analysis.

In order to understand phase transformation of the as-synthesized powders during the heat treatment, a differential thermal analysis was performed for the as-synthesized powders. The thermal analysis results of the as-synthesized $x=0.5$ powders are shown in Fig. 3. The DSC/TG curves show a weight loss of $\sim$16%, accompanied by the two exothermic peaks at $\sim$285 °C and 392 °C. Weight loss of $\sim$10% at temperatures below 370 °C is attributed to the decomposition of the residual organic complex. A exothermic peak occurred at $\sim$392 °C, accompanied by a small weight loss of $\sim$6%, which is caused by the chemical reaction of $Mg(OH)_2$, $MgTiO_3$ and $Ba_6Ti_{17}O_{40-x}$.

XRD patterns of the $(1-x)Ba_{0.5}Sr_{0.5}TiO_3$–$xMg_2TiO_4$ composite ceramics sintered at different temperatures are shown in Fig. 4. All samples sintered at 1200 °C show a multiphase structure of BST, $BaMg_6Ti_6O_{19}$, Mg_2TiO_4 and

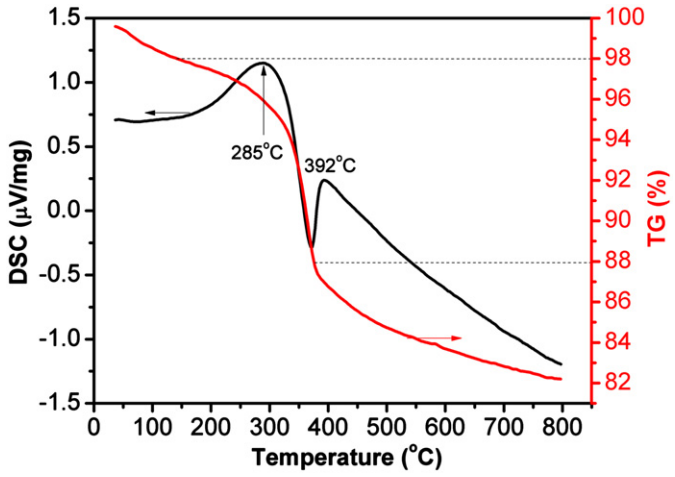

Fig. 3. DSC/TG curves of the $(1-x)Ba_{0.5}Sr_{0.5}TiO_3$–$xMg_2TiO_4$ ($x=0.5$) powders synthesized by the hydrothermal method.

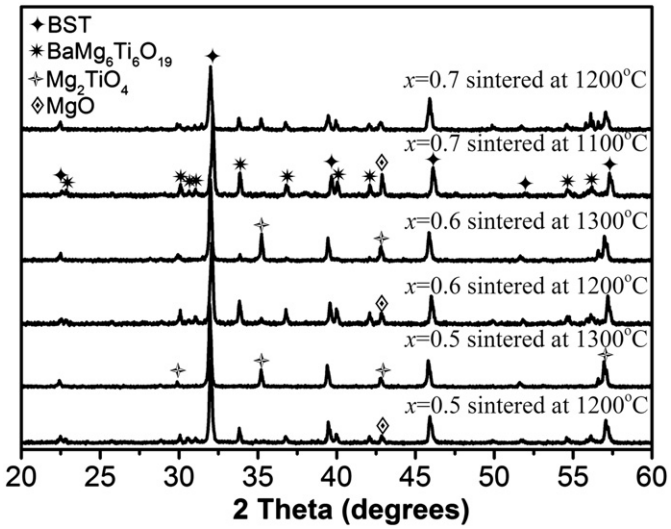

Fig. 4. XRD patterns of the $(1-x)Ba_{0.5}Sr_{0.5}TiO_3$–$xMg_2TiO_4$ composites sintered at different temperatures for 4 h.

MgO. As the sintering temperature increases, $BaMg_6Ti_6O_{19}$ and MgO diffraction peaks are gradually weakened and even disappeared, while Mg_2TiO_4 diffraction peaks are gradually increased. The sample with $x=0.5$ sintered at 1300 °C shows a bimodal composition of BST and Mg_2TiO_4, whereas those with $x=0.6$ sintered at 1300 °C have additional $BaMg_6Ti_6O_{19}$ diffraction lines. The sample with $x=0.7$ sintered at 1200 °C is very fragile, so XRD pattern of those with $x=0.7$ sintered at 1100 °C is also given. Crystal structure of the sample with $x=0.7$ sintered at 1100 °C is in accordance with that of the sample with $x=0.5$ sintered at 1200 °C. Compared with the conventional solid-state route [4], the $Ba_{0.5}Sr_{0.5}TiO_3$–Mg_2TiO_4 composites prepared by the hydrothermal method have low sintering temperature.

Fig. 5 shows the cross-section SEM images of $(1-x)Ba_{0.5}Sr_{0.5}TiO_3$–$xMg_2TiO_4$ composites sintered at different temperatures. The sample with $x=0.5$ sintered at 1200 °C has a multimodal microstructure, consisting of claviform grains, fine grains and large grains. As the sintering temperature increases, grain size increases and the sample's microstructure becomes dense. When sintered at 1300 °C, the sample's microstructure becomes a bimodal, consisting of fine grains with size of 0.5–1.5 μm and vermiculate-shaped grains of 3–5 μm. At the same sintering temperature, grain size increases and the sample's microstructure becomes dense with increasing the concentration of Mg_2TiO_4. The microstructure of the sample with $x=0.7$ sintered at 1100 °C is similar to that of the sample with $x=0.5$ sintered at 1200 °C.

Fig. 6 shows temperature dependent permittivity of the $(1-x)Ba_{0.5}Sr_{0.5}TiO_3$–$xMg_2TiO_4$ composites sintered at different temperatures for 4 h. As the sintering temperature increases, the dielectric anomalous peaks of the samples with $x=0.5$ and 0.6, corresponding to the cubic-tetragonal

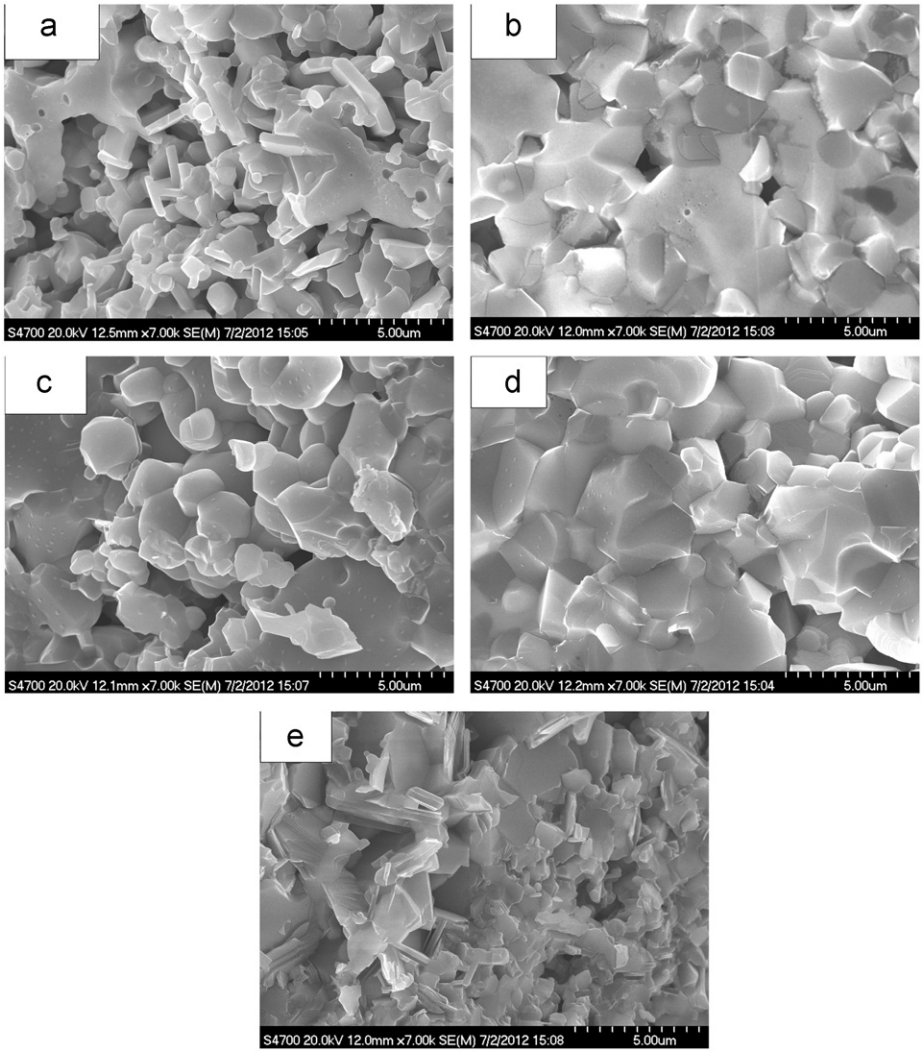

Fig. 5. Cross-section SEM images of the $(1-x)Ba_{0.5}Sr_{0.5}TiO_3$–$xMg_2TiO_4$ composites sintered at different temperatures for 4 h: (a) $x=0.5$ sintered at 1200 °C, (b) $x=0.5$ at 1300 °C, (c) $x=0.6$ at 1200 °C, (d) $x=0.6$ at 1300 °C and (e) $x=0.7$ at 1100 °C.

phase transition, are markedly enhanced and sharpened. The enhancement and sharpening is due to the increase in the density and grain size. Meanwhile, their maximum permittivity temperature T_m (T_C) is increased. The increase in T_C is caused by the increase of Ba/Sr ratio in BST resulting from the decrease of $BaMg_6Ti_6O_{19}$ phase (shown in Fig. 4). As the concentration of Mg_2TiO_4 increases, the dielectric peaks of the cubic-tetragonal phase transition are markedly suppressed. Interestingly, for the sample with $x=0.7$ sintered at 1100 °C, a dielectric abnormity represented by enhancing dielectric response with increasing temperature at above 80 °C is observed. To understand the dielectric abnormity and temperatures dependent permittivity of the sample with $x=0.7$ measured at different frequencies is displayed in Fig. 6(c). The dielectric abnormity is markedly suppressed with increasing frequency, indicating that the dielectric abnormity is attributed to the low density of the sample.

The samples sintered at the optimizational sintering process are chose to investigate their tunable and microwave properties. DC bias field dependent permittivity of the $(1-x)Ba_{0.5}Sr_{0.5}TiO_3$–$xMg_2TiO_4$ composites at 20 °C and 10 kHz is shown in Fig. 7. Their dielectric properties and calculated tunabilities are summarized in Table 1. As the concentration of Mg_2TiO_4 increases, the tunability decreases. This is because that the relative content of BST ferroelectric phase decreases and the connectivity between BST–BST grains weakens with increasing the concentration of Mg_2TiO_4. The tunability of the sample with $x=0.7$ is less than 5.0%, which is possible due to the fact that the T_C (shown in Table 1) of the sample is too low [12] and the relative content of BST phase is too small.

Microwave dielectric parameters measured at room temperature are listed in Table 1. As the concentration of Mg_2TiO_4 increases, permittivity decreases, whereas Q ($Q=1/\tan\delta$) value firstly increases and then decreases. For microwave dielectrics, polarizability dominates permittivity [19]. As the concentration of Mg_2TiO_4 increases, average ionic polarizability decreases, thus decreasing permittivity. The intrinsic loss strongly depends on permittivity. The sample

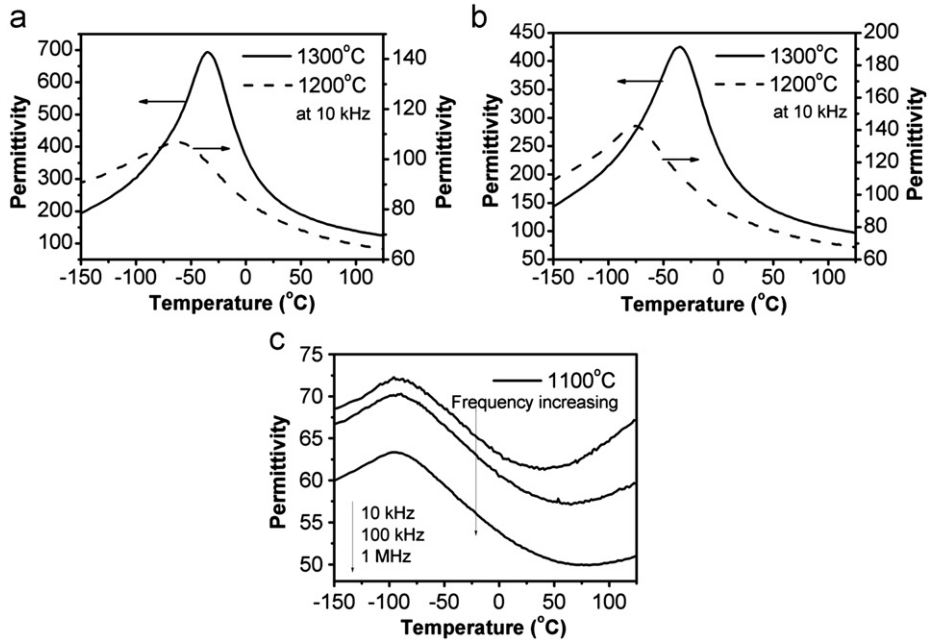

Fig. 6. Temperature dependent permittivity of the $(1-x)Ba_{0.5}Sr_{0.5}TiO_3$–$xMg_2TiO_4$ composites sintered at different temperatures for 4 h: (a) $x=0.5$ sintered at 1200 °C and 1300 °C, (b) $x=0.6$ at 1200 °C and 1300 °C and (c) $x=0.7$ at 1100 °C.

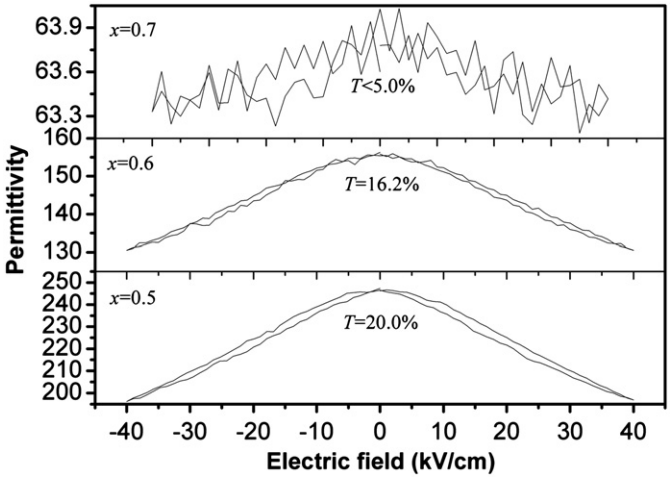

Fig. 7. DC bias field dependence of permittivity of the $(1-x)Ba_{0.5}Sr_{0.5}TiO_3$–$xMg_2TiO_4$ composites.

Table 1
Microwave and dielectric properties of the $(1-x)Ba_{0.5}Sr_{0.5}TiO_3$–$xMg_2TiO_4$ composites.

Ceramic samples	Dielectric properties (at 10 kHz)				Microwave properties		
	T_C (°C)	At about 20 °C		Tunability (40 kV/cm) (%)	Resonant frequency (GHz)	ε (at resonant frequency)	Q value
		ε	tanδ				
$x=0.5$	−35	266	0.012	20.0	3.369	200	287
$x=0.6$	−35	180	0.009	16.2	3.804	136	342
$x=0.7$	−92	61	0.047	< 5.0	6.324	48	148

with $x=0.7$ has low Q value, which may be related to the low density of the sample. Compared with the conventional "two step" method [4], the $Ba_{0.5}Sr_{0.5}TiO_3$–Mg_2TiO_4 composites with $x=0.5$ and 0.6 prepared in situ by the hydrothermal method have high Q value, probably due to the low residual stress between BST phase and dielectric phase [20].

4. Conclusions

Hydrothermal synthesized $(1-x)Ba_{0.5}Sr_{0.5}TiO_3$–$xMg_2TiO_4$ powders showed a multiphase structure of BST, $Mg(OH)_2$, $MgTiO_3$ and $Ba_6Ti_{17}O_{40-x}$. After sintered at temperatures below 1300 °C, biphase $Ba_{0.5}Sr_{0.5}TiO_3$–Mg_2TiO_4 composite ceramics were successfully formed. The dielectric peaks of the cubic-tetragonal phase transition of the samples with $x=0.5$ and 0.6 were markedly enhanced and sharpened and shifted toward high temperature with increasing the sintering temperature. As the concentration of Mg_2TiO_4 increased, both permittivity and tunability decreased, whereas Q value firstly increased and then decreased. The sample with $x=0.6$ had good dielectric properties, with ε of 136, Q of 342 (at 3.804 GHz) and T of 16.2%, which is promising candidate for potential tunable microwave devices for wireless communication applications.

Acknowledgments

This research was financially supported by the Ministry of Science and Technology of China through 973-Project

under Grant no. 2009CB623302, the Natural Science Foundation of China (Grant no. 51202234), China Postdoctoral Science Foundation (No. 20110490695) and the Opening Project of Shanghai Key Laboratory of Special Artificial Microstructure Materials and Technology (ammt2012A-7).

References

[1] A.K. Tagantsev, V.O. Sherman, K.F. Astafiev, J. Venkatesh, N. Setter, Ferroelectric materials for microwave tunable applications, Journal of Electroceramics 11 (1) (2003) 5.

[2] L. Sengupta, S. Sengupta, Breakthrough advances in low loss, tunable dielectric materials, Materials Research Innovations 2 (5) (1999) 278.

[3] Y. Chen, X.-L. Dong, R.-H. Liang, J.-T. Li, Y.-L. Wang, Dielectric properties of $Ba_{0.6}Sr_{0.4}TiO_3/Mg_2SiO_4$/MgO composite ceramics, Journal of Applied Physics 98 (6) (2005) 064107.

[4] X. Chou, J. Zhai, X. Yao, Dielectric tunable properties of low dielectric constant $Ba_{0.5}Sr_{0.5}TiO_3$–Mg_2TiO_4 microwave composite ceramics, Applied Physics Letters 91 (12) (2007) 122908.

[5] Q. Zhang, J. Zhai, X. Yao, Low loss high tunability of $Ba_{0.4}Sr_{0.6}TiO_3$–$Mg_3B_2O_6$ microwave composite ceramics, Journal of the American Ceramic Society 93 (9) (2010) 2560.

[6] M. Zhang, J. Zhai, X. Yao, Microwave dielectric properties of high dielectric tunable-low permittivity $Ba_{0.5}Sr_{0.5}TiO_3$–$Mg_2(Ti_{0.95}Sn_{0.05})O_4$ composite ceramics, Ceramics International 38 (Suppl. 1) (2012) S173.

[7] R.H. Liang, X.L. Dong, Y. Chen, F. Cao, Y.L. Wang, Improvement of microwave loss tangent and tunability of $Ba_{0.55}Sr_{0.45}TiO_3$/MgO composites using the heterogeneous precipitation method, Journal of the American Ceramic Society 89 (10) (2006) 3273.

[8] T. Wang, F. Gao, G. Hu, C. Tian, Synthesis $Ba_{0.6}Sr_{0.4}TiO_3$–$ZnNb_2O_6$ composite ceramics using chemical coating method, Journal of Alloys and Compounds 504 (2) (2010) 362.

[9] U.C. Chung, C. Elissalde, M. Maglione, C. Estournes, M. Pate, J.P. Ganne, Low-losses, highly tunable $Ba_{0.6}Sr_{0.4}TiO_3$/MgO composite, Applied Physics Letters 92 (4) (2008) 042902.

[10] Q. Xu, X.-F. Zhang, H.-X. Liu, W. Chen, M. Chen, B.-H. Kim, Effect of sintering temperature on dielectric properties of $Ba_{0.6}Sr_{0.4}TiO_3$–MgO composite ceramics prepared from fine constituent powders, Materials & Design 32 (3) (2011) 1200.

[11] J. Zhang, J. Zhai, X. Chou, X. Yao, Relaxor behavior and dielectric properties of $(1-x)Ba_{0.6}Sr_{0.4}TiO_3-xMg_{0.7}Zn_{0.3}TiO_3$ composite ceramics for tunable microwave applications, Solid State Communications 147 (9–10) (2008) 392.

[12] J. Zhang, J. Zhai, H. Jiang, X. Yao, Raman and dielectric study of $Ba_{0.4}Sr_{0.6}TiO_3$–$MgAl_2O_4$ tunable microwave composite, Journal of Applied Physics 104 (8) (2008) 084102.

[13] J. Zhang, J. Zhai, J. Wang, J. Shao, X. Lu, X. Yao, Infrared dielectric response and Raman spectra of tunable $Ba_{0.5}Sr_{0.5}TiO_3$–Mg_2TiO_4 composite ceramics, Journal of Applied Physics 107 (1) (2010) 014106.

[14] L. Qiu, R. Xie, P. Ding, B. Qu, Preparation and characterization of $Mg(OH)_2$ nanoparticles and flame-retardant property of its nanocomposites with EVA, Composite Structures 62 (3–4) (2003) 391.

[15] M. Zheng, X. Xing, J. Deng, L. Li, J. Zhao, L. Qiao, C. Fang, Synthesis and characterization of (Zn, Mn)TiO_3 by modified sol–gel route, Journal of Alloys and Compounds 456 (1–2) (2008) 353.

[16] Y. Murakami, T. Matsumoto, Y. Takasu, Salt catalysts containing basic anions and acidic cations for the sol–gel process of titanium alkoxide: controlling the kinetics and dimensionality of the resultant titanium oxide, The Journal of Physical Chemistry B 103 (11) (1999) 1836.

[17] K. Nakamoto, Infrared and Raman Spectra of Inorganic and Coordination Compounds, New York, 1970.

[18] L. Wang, H. Kang, D. Xue, C. Liu, Synthesis and characterization of $Ba_{0.5}Sr_{0.5}TiO_3$ nanoparticles, Journal of Crystal Growth 311 (3) (2009) 605.

[19] M. Reaney, I. David, Microwave dielectric ceramics for resonators and filters in mobile phone networks, Journal of the American Ceramic Society 89 (7) (2006) 2063.

[20] K.S. Kim, S.H. Shim, S. Kim, S.O. Yoon, Low temperature and microwave dielectric properties of TiO_2/ZBS glass composites, Ceramics International 36 (5) (2010) 1571.